POLITECNICO
MILANO 1863

SCUOLA DI INGEGNERIA INDUSTRIALE
E DELL'INFORMAZIONE

Executive Summary of the Thesis

Data-Driven Modeling of the Flow Field Between Two PWR Surrogate Bundles Under Seismic Conditions Using Bagging-Optimized Dynamic Mode Decomposition (BOP-DMD)

Laurea Magistrale in Nuclear Engineering - Ingegneria Nucleare

Author: Haidy Ibrahim

Advisor: Prof. Antonio Cammi

Co-advisors: Carolina Introini, Roberto Capanna

Academic year: 2022-2023

1. Introduction

A typical Pressurized Water Reactor (PWR) core is composed of several fuel assemblies (heat source) around which water flows (heat drain) to moderate the neutron flux and cool down the fuel assemblies. Disturbances to the nominal fluid flow patterns, for example, due to natural catastrophes such as earthquakes, could highly affect the criticality of the reactor core and accordingly its safe operation. The typical spacing between the reactor fuel rods in each assembly is around 3 mm: during an earthquake, vibrations may cause two fuel rods of coming into contact and thus disturb the moderator axial flow. Hence, the study of flow field patterns and fluid-structure interactions (FSI) under seismic conditions is of high importance to guarantee the safe operation of the reactor even under these extreme conditions. Typically, moderator flow patterns and parameters are studied using vendor-specific design codes which are usually either 1D models based on best estimate system analysis or, in some cases, CFD analysis integrated with 3D CAD models. While 1D codes exhibit some limitations when studying local effects and disturbances, CFD codes are quite accurate but very expensive for modeling and computational POV. Experimental measuring techniques like Particle Image Velocimetry (PIV) have been applied and shown great success [1].

PIV has shown many advantages, among which are its usability between fuel bundles in tide geometries, its capability of resolving the velocity field into its components, and its relatively low computational cost. The key working principle is to make the fluid motion visible and that involves three major steps: 1) feed the flow with seed particles that are light reflecting; 2) illuminate the flow with a light sheet (typically a laser sheet); 3) record particle movements using cameras. In this study, we treat data obtained from the deployment of time-resolved PIV between two PWR surrogate bundles [1]. Being a time-resolved data measurement technique makes it ideal for our study since our final goal is to use the measured data to achieve field reconstruction and forecasting. Such measurements are interpreted using a cross-correlation algorithm and stored in high-dimensional arrays. Those high-dimensional data arrays are not easy to an-

alyze and the use of model reduction techniques is highly important.

When modeling complex systems, is useful to reduce them to a tractable form i.e. achieve low dimensionality. This is usually done through the use of model-based algorithms that relies primarily on the projection onto low-dimensional subspaces of the system's governing equations to follow its dynamics. However, in situations where the governing equations are not known or not well formulated, the use of Data-Driven Models (DDM) is preferred. In such models, the knowledge of the system's underlying equations is not a necessity. An example of such an approach is Dynamic Mode Decomposition (DMD). To model a system using DMD the only requirement is to have a series of snapshots, either coming from some high-fidelity model or directly from experimental data, of the system's variables of interest, taken at points in time, dense enough to resolve the transient dynamics of interest [2]. The algorithm decomposes the dataset into a group of low-dimensional dynamic modes, that can then be used to map the entire system and for future data prediction.

The main challenge faced when treating high-dimensional data is the need for model-reduction techniques that can overcome the presence of measurement noise and are capable of field reconstruction and forecasting. Unfortunately, DMD is highly biased to noise, and in its standard form it can only treat clean or weakly noised data: as the noise in the measurements increases, the algorithm fails to capture the system dynamics [4]. In our study, we used an enhancement to the exact DMD algorithm known as Bagging-Optimized Dynamic Mode decomposition (BOP-DMD) [4]. The study presented in this paper includes applying the BOP-DMD algorithm to velocity fields for the purposes of reconstruction and forecasting, comparing the obtained results to those from exact DMD. Additionally, the different fields were investigated in the presence of noise and after de-noising to study the effect of noise on reconstruction. The study confirms the reliability of the BOP-DMD technique in the reconstruction and future prediction of high-dimensional field behavior.

2. Dynamic Mode Decomposition

One of the most recent data-driven modeling techniques is dynamic mode decomposition (DMD), which can be considered as a combination in its formulation of the proper-orthogonal decomposition (POD), and Fourier transforms [2]. The former is a spatial reduction technique while the latter is a transform in the time domain. In this subsection, we will try to briefly explain the algorithm behind the DMD [2].

Any dynamical system can be represented by the following non-linear relation:

$$dX/dt = F(x,t) \tag{1}$$

x is measurable in time and belongs to the high dimensional space $\mathcal{R}^n$. The goal is to approximate this nonlinear system into an easier-solvable linear one. Hence equation 1 can be rewritten as

$$dX/dt = AX \tag{2}$$

If we assume that X satisfies the Eigenvalue problem $X = \gamma \exp \lambda t$, and $\lambda\gamma = A\gamma$, then its solution can be obtained with a simple knowledge of the initial condition X_0

$$X(t) = \sum_{k=1}^{n} \phi_k \exp(\omega_k t) b_k = \Phi \exp(\Omega t) b \tag{3}$$

where ϕ_k and ω_k are the eigenvectors and eigenvalues of the matrix A, and b_k is the loading of the initial X_0. Mathematically speaking, the architecture of the DMD is based on finding the operator that maps our data matrix X from a current state in time to its future projection, such that

$$X_{k+1} = \mathcal{A} X_k \tag{4}$$

$\mathcal{A}$ is the mapping matrix, it is a linear time-independent operator having the same dimensions of the data matrix X, and it has the capability of mapping matrix X from a current state K to a future state $K+1$ Where

$$\mathcal{A} = \exp(A\Delta t) \tag{5}$$

and the solution to the system can be expressed in terms of the eigenvalues λ_k and the eigenvectors ϕ_k of the mapping matrix $\mathcal{A}$ as

$$X_k = \sum_{j=1}^{r} \phi_j \lambda_j^k b_j = \Phi \Omega^k b \tag{6}$$

Such that the first mode can be expressed as $X_1 = \Phi b$. Hence, the DMD algorithm finds a mapping matrix that maintains a least square fit

$$||X_{k+1} - \mathcal{A}X_K||_2 \quad (7)$$

A full description of the DMD architecture can be found in the book of *Dynamic Mode Decomposition* by Kutz [2].
The DMD method is highly successful in data reconstruction and forecasting, however, as mentioned above, it has some limitations; it allows noise propagation, and hence if dealing with highly noised data DMD fails to capture system dynamics.

3. Bagging-Optimized Dynamic Mode Decomposition

Since fluid field measurements could be highly noisy, the use of regular DMD is not much reliable, as it has shown a biased behavior towards noise which makes accurate data reconstruction impossible. An enhancement has been made to the exact DMD algorithm to make it capable of the analysis of noisy fields, known as bagging-optimized dynamic mode decomposition (BOP-DMD). This data-driven modeling technique depends on the statistical method of bagging which improves the forecasting accuracy of DMD even in the presence of noise and provides uncertainty quantification for the reconstructed fields. As an ensemble method, bagging is a variance reduction technique for a given process that may involve variable selection or linear fitting. Following [4] the algorithm was developed by Sashidhar and Kutz as a modification to a previously developed one (optimized DMD) featuring three additional characteristics: 1) initialization procedure to stabilize the variables projection algorithm; 2) statistical bagging scheme to reduce variance and stabilize the models; 3) uncertainty quantification for temporal and spatial profiles. These three features make BOP-DMD a successful DDM for highly noisy data and high-dimensional fields.
The input for the BOP-DMD algorithm is the original data matrix X, the number of trials k, and the randomly selected indices p. First, the Opt-DMD algorithm is run on the full data matrix to get the eigenvalues λ_{opt} which will be used as initial conditions for the BOP-DMD algorithm. Using this initial condition, the algorithm is run for k trials to obtain subsets of the original data matrix X(k) which are generated by choosing p randomly selected column indices of the original data matrix X. At this point, bagging is introduced and the obtained eigenvalues λ_k, DMD modes ϕ_k, and their loadings b_k are used as initial conditions [4]. Once the final eigenvalues, DMD modes, and their loadings are obtained, the algorithm proceeds similarly to that of the exact DMD discussed in 2.

4. Experiment

The data used in this analysis is obtained from the ICARE experimental facility, the experiment involved the implementation of the PIV technique explained earlier to the fluid field understudy to obtain field measurements. A detailed description of the experimental facility is presented by Capanna and Longo in [1]. In the experiment, the flow was loaded with the high florescent seed particles, and the motion of those particles is used to calculate field parameters such as velocity and vorticity. The flow was illuminated using the thin laser sheets which were carefully introduced in between bundles to allow visualization of field motion in the tide geometry. The motion is recorded using a sampling time of 2 seconds per cycle: the optical axis was kept in between bundles and the camera was allowed to move axially. Multiple runs were recorded to increase the number of forcing cycles and achieve statistical convergence. The bundles are excited using the hydraulic jack at a 5 Hz frequency with an excitation amplitude of 1.7 mm, resulting in fluctuations in the velocity field due to bundle movement. The PIV cross-correlation algorithm is DAVIS 10.3 from LaVision, Inc. with an interrogation window of 32 by 32 pixels allowing a spatial resolution of 0.4 mm. It should be noted here that there is a level of uncertainty in the obtained data from the lack of use of a calibration target and hence, the results obtained from the experiment are treated as qualitative [1].

5. Methodology and Results

5.1. Data acquisition and treatment

The analysis includes four different experiments where the difference between each is in the ex-

citation amplitude and frequency: the first experiment is at an excitation of 0.5 mm at 3 Hz; the second is at an excitation of 0.5 mm at 8.06 Hz; the third is at an excitation of 1.7 mm at 1 Hz; and the fourth is at an excitation of 1.7 mm at 14 Hz. The measurements are recorded in a 3D matrix having the size x-coordinate by y-coordinate by time steps (46-by-42-by-12812). The measured parameters are; the instantaneous transversal velocity, instantaneous axial velocity, transversal velocity unaveraged, axial velocity unaveraged, the vorticity of the velocity field, and the Turbulent Kinetic Energy (TKE), each recorded in each cell of the domain and for each time step. In our analysis, we will only discuss in detail the axial velocity field from the first experiment (excitation of 0.5 mm at 3 Hz) for the sake of brevity and we will display results obtained from the analysis of the other fields for comparison. The code used in this analysis is the BOP-DMD code developed and run using MATLAB. First, we start by applying singular value decomposition (SVD) to the data matrix (V_y) to obtain the number of modes to which we will reduce our problem and obtain the best fit. To decide the dimensionality of the low-dimensional space, we use the eigenmodes of the matrix vs. the inverse of their energy content as shown in Figure 1: for our purposes, an acceptable number of modes is the one achieving around 90% energy content, and in our case, it was found to be 3 modes. The number of cycles (trials) and the number of the randomly selected column indices were decided to be 100 and 50 respectively: the choice of both values was arbitrarily based on a trial and error basis to achieve the best fit at the lowest computational cost possible. It should be noted here that non-linearities in the treated data were ignored. Also, the use of the BOP-DMD algorithm doesn't require a monotonous hyper-parameter search process, only the choice of the rank using SVD was necessary, and the rest of the parameters (ex; time step) were arbitrary due to the analysis of experimental data. The optimized-DMD code was first to run to obtain initial values of the DMD eigenvalues, DMD modes, and their loadings which act as seeding fed to the BOP-DMD algorithm. The algorithm was then run for several cycles: at each cycle, it updates the seeding parameters, and by the final cycle improved DMD eigenvalues, modes, and loadings are obtained. The algorithm proceeds similarly to the exact DMD where a distribution for forecasting and reconstruction is obtained. It should be noted here that since we are dealing with highly noised fields, we use the fast Fourier transform for de-noising to obtain better results (as will be discussed in the following). Validation is performed by comparing the reconstructed field to the experimental one.

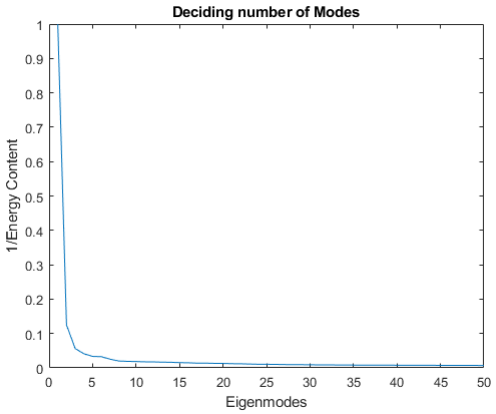

Figure 1: Eigenmodes of the instantaneous transversal velocity V_y V.s. the inverse of their energy content

5.2. Reconstruction and validation

The reconstructed field satisfies equation 6. Here the DMD eigenvalues, DMD modes, and their loadings are taken to be the mean values over the single DMD eigenvalues, DMD modes, and their loadings obtained from each cycle. It should be noted here that the reconstructed field can later be used as a training data matrix for achieving accurate forecasting. Validation is done by comparing the reconstructed field to the original field of axial velocity. The comparison was performed in a 2D plot as shown in Figure 2. The figure shows the axial velocity field taken at a fixed time point (T=1). The blue lines represent the original data field, while the red lines represent the reconstructed one using BOP-DMD. The plot shows a null axial velocity field at the peripheral regions and then follows a decreasing behavior and then a semi-constant one at mid-regions. The semi-constant behavior is quite reasonable since the plot was taken at an initial time point where the flow field wouldn't have acquired enough momentum to show variations in its axial velocity. The figure also shows that both the original and reconstructed fields

follow the same trend however a variation is present in the mid-regions.

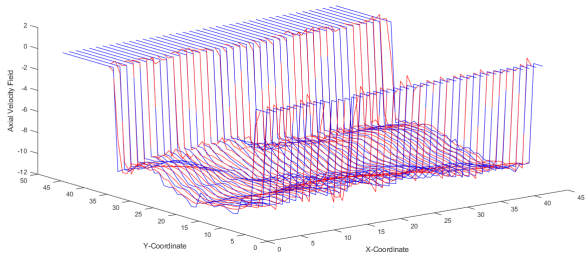

Figure 2: 2D plot of the reconstructed axial velocity and the experimental one at T=1, Y=1

Figure 3 shows the reconstructed field and the original field after removing the noise compared at different time steps and positions. Denoising was performed using a fast-Fourier transform and was confirmed using wavelet analysis. By studying the plot shown in Figure 3, the sharp decrease in the peripheral regions is now smoother. Also, the reconstructed field is not completely constant in the mid-regions but experiences some level of small variations. Figure 3 also shows the axial velocity field (reconstructed and original) fixed at Y=10 and T=10: the discrepancies between both the reconstructed and the original field at different time steps and positions have experienced serious reductions ranging from 0.2% up to 6.5% which is almost half of those in the presence of noise.

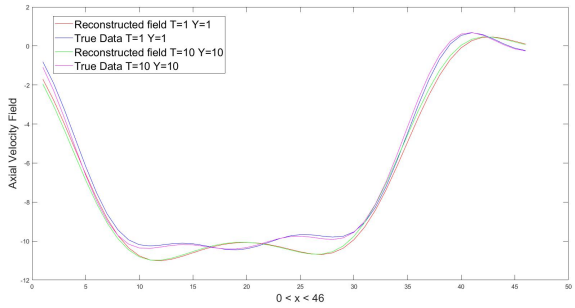

Figure 3: Line plot of the reconstructed axial velocity field and the original field after de-noising at T=1, Y=1, and T=10 Y=10

6. Efect of Noise

It is evident that the presence of noise can affect the accuracy of the reconstructed field. For the exact DMD, the algorithm fails to capture system dynamics at final time points, while for BOP-DMD the presence of noise increased variations between both reconstructed and original fields to two times its value without noise. Figure 4 shows both reconstructed and original fields in the presence of noise and after de-noising; clearly, the reconstructed field shows better agreement with the original field after de-noising was done, the advancement of FFT as a noise filtering technique is that it smoothens the signal and removes fluctuations (noise) while barely causing any distortion to the original field.

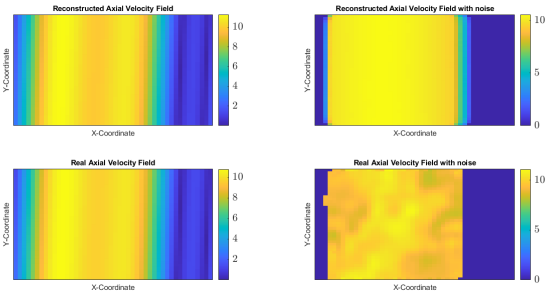

Figure 4: Reconstructed and original fields in the presence of noise (right) and after de-noising (left)

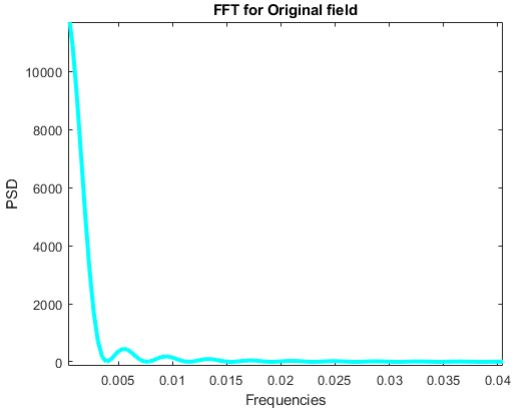

Figure 5: PSD vs. Frequencies for the axial velocity field

For the treated data in this study, the noise is either systematic from the measuring equipment or arbitrary due to the lack of use of a calibration target during the experiment. In all cases, de-noising of the reconstructed fields was performed using FFT (fast-Fourier transform). Figure 5 shows the PSD (power spectral density) plotted against the frequencies, we can see the minor peaks following the central peak, those

small peaks represented noise and were cut out.

7. Results from Other Fields

The analysis also included other fields, for example, the transversal instantaneous velocity was studied and is shown in Figure 6 where the reconstructed field is plotted against the original field after de-noising using FFT.

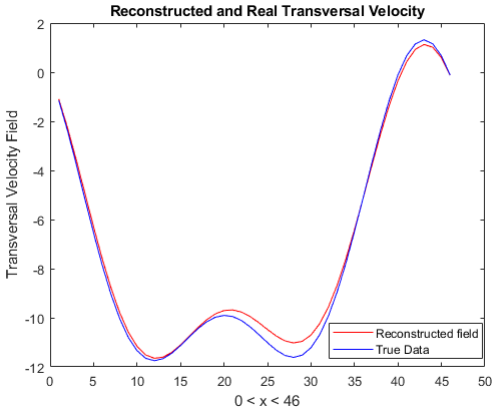

Figure 6: Reconstructed and real transversal velocity field

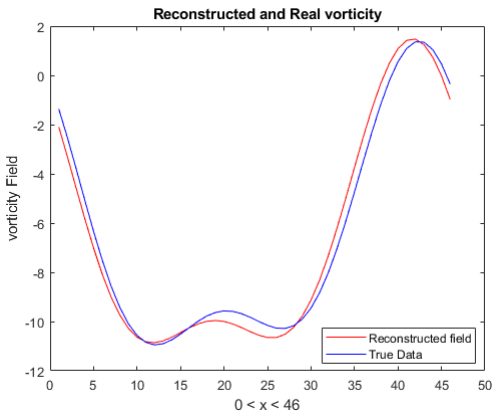

Figure 7: Reconstructed vorticity

This analysis also included the reconstruction of the vorticity field. The vorticity reconstruction process involved using the fabricated axial and transversal velocity fields obtained from the BOP-DMD reconstruction algorithm. Following equation 8 the vorticity field Ω is given by the curl of the velocity field U.

$$\Omega = \nabla \times U \tag{8}$$

The reconstructed vorticity was compared to the original vorticity field obtained from direct measurement both after de-noising and are shown in Figure 7.

8. Conclusions

The BOP-DMD method when used for data reconstruction of high-dimensional fields shows a high level of accuracy. In this study, the method was tested on high-dimensional and highly noised fields and has proven its superiority over the exact DMD method. Also, the method is relevant for any high-dimensional field and does not require tedious hyperparameter tuning, it can be used for future data prediction and can highly reduce the computational cost when treating high-dimensional complex fields, which we intend to use as part of future work. The use of a noise filtering technique on the reconstructed fields (FFT or wavelets analysis) can highly enhance reconstruction accuracy, especially when dealing with systematic noise. Another helpful approach, that was not presented here, is to apply FFT to the training data. Alternatively, noise can be studied through another approach named "DMD with control" as in the work of Proctor, Brunton, and Kutz [3] which can be studied in future works.

References

[1] Roberto Capanna, Lorenzo Longo, Fabienne Bazin, Guillaume Ricciardi, and Philippe M Bardet. Deployment of time-resolved particle image velocimetry between two pwr surrogate bundles. *Nuclear Engineering and Design*, 382:111375, 2021.

[2] J Nathan Kutz, Steven L Brunton, Bingni W Brunton, and Joshua L Proctor. *Dynamic mode decomposition: data-driven modeling of complex systems*. SIAM, 2016.

[3] J Nathan Kutz, Steven L Brunton, Bingni W Brunton, and Joshua L Proctor. *Dynamic mode decomposition: data-driven modeling of complex systems*. SIAM, 2016.

[4] Diya Sashidhar and J Nathan Kutz. Bagging, optimized dynamic mode decomposition for robust, stable forecasting with spatial and temporal uncertainty quantification. *Philosophical Transactions of the Royal Society A*, 380(2229):20210199, 2022.